ARTICLE IN PRESS

Available online at www.sciencedirect.com

SCIENCE DIRECT®

Aerosol Science III (IIII) III–III

Journal of Aerosol Science

www.elsevier.com/locate/jaerosci

Reduction of the condensation/evaporation dynamics for atmospheric aerosols: Theoretical and numerical investigation of hybrid methods

Edouard Debry, Bruno Sportisse*

CEREA, Teaching and Research Center in Atmospheric Environment, Joint Laboratory Ecole Nationale des Ponts et Chaussées/Electricité de France R&D, 8 rue Blaise Pascal, 77455 Champs sur Marne, France

Received 25 June 2004; received in revised form 29 September 2005; accepted 29 September 2005

Abstract

The dynamical behaviour of atmospheric aerosols is characterized by a wide range of timescales, especially due to the fast growth of small particles through condensation/evaporation. The resulting models are particularly stiff and their numerical simulation still remains a challenge. Some techniques based on the assumption of condensation/evaporation equilibrium are usually advocated in order to circumvent these difficulties.

The objective of this article is to investigate the different approaches on a theoretical basis. The appropriate framework is the theory of reduction for slow/fast models, for which many tools are already available. The application to aerosol modelling leads to the so-called hybrid methods. We also propose a hierarchy of reduced models and compare some numerical algorithms in a box model simulation for inorganic species.

Keywords: Aerosol modelling; Particles; GDE; Condensation/evaporation; Mass transfer; Reduction; Hybrid models; Equilibrium; Dynamic; Lagrangian models; Bins; Bulk; Size-resolved models; Slow/fast species; Lumping; Thermodynamic model; Isorropia; Inorganics

0. Introduction

The accurate modelling of aerosol dynamics is a crucial issue in atmospheric sciences for many reasons

- small particles may have a direct impact on health and as such are a key component for air pollution models: the smallest particles are supposed to have the most adverse effect;
- the coupling with gas-phase through condensation/evaporation may modify the gas-phase concentrations and depends on the size distribution and chemical composition;
- at larger scales, the (direct) radiative impact of aerosols is still uncertain and is strongly related to the size distribution and chemical composition of aerosols;

* Corresponding author. Tel.: +33 1 64 15 21 41; fax: +33 1 64 15 21 70.
E-mail address: bruno.sportisse@cerea.enpc.fr (B. Sportisse)
URL: http://www.enpc.fr/cerea/ (B. Sportisse).

0021-8502/$ - see front matter © 2005 Elsevier Ltd. All rights reserved.
doi:10.1016/j.jaerosci.2005.09.004

Nomenclature

Aerosol modelling

m	mass of aerosol
m_0	smallest aerosol mass
x	logarithm of m
n	number distribution
q_i	aerosol density distribution for species X_i
c_i^{g}	gas-phase concentration of species X_i
$I_i(m,t)$	c/e mass flux for species X_i to aerosols of mass m
$I_0(m,t)$	growth rate of aerosols of mass m ($\sum_{i=1}^{i=n_{\mathrm{s}}} = I_0$)
H_0	growth rate in logarithmic scale (I_0/m)
K_i	total mass (aerosol phase and gas phase) for species X_i
c_i^{g}	gas-phase concentration for species X_i
c_i^{eq}	surface concentration for species X_i (given by an equilibrium model in the "reverse mode")

Sectional lagrangian formulation

n_{b}	number of bins
$\bar{x}^j$	lower bound of bin j defined as $[\bar{x}^j, \bar{x}^{j+1}]$
N^j	integrated number distribution over bin j
Q_i^j	integrated aerosol density distribution for species X_i over bin j
$\tilde{m}_i^j$	average mass of species X_i in bin j (Q_i^j/N_j)
$\tilde{m}^j$	total (for all species) average mass in bin j ($\sum_{i=1}^{i=n_{\mathrm{s}}} \tilde{m}_i^j$)
$\tilde{x}^j$	corresponding logarithm
τ_i^j	timescale of species X_i in bin j
d_p^j	average aerosol diameter for bin j
I_i^j	mass flux for species i in bin j

Reduction

z_{s} (z_{f})	slow (fast) components
ε	ratio of fast timescales to slow timescales
J	Jacobian matrix
λ_k	kth eigenvalue of the Jacobian matrix
u_k	kth eigenvector
p_{s} (p_{f})	projection to the slow (fast) subspace
I_{QSSA}	QSSA ratio
ε_c	criterion for defining the QSSA ratio
d_{c}	cut-off diameter used for hybrid models
j_{c}	cut-off index of bins for hybrid models
λ_{c}	cut-off eigenvalue for hybrid models

- through cloud condensation on existing particles (the cloud condensation nuclei), which is strongly related to the size and composition as well, the aerosols also have an (indirect) effect for the radiative state of the atmosphere.

The aerosol dynamics is based on the so-called general dynamic equation (GDE) for aerosols, which describes the time evolution of the particle size distribution and of the chemical composition in a well stirred tank reactor. This corresponds in practice to a grid cell of a three-dimensional eulerian Chemistry-Transport Model.

The processes to be described are nucleation, (brownian) coagulation and condensation/evaporation (gas to particle conversion). We refer for instance to Seinfeld and Pandis (1998) for a general presentation.

The numerical simulation of the GDE is still a challenging point in current Chemistry-Transport Models: the resulting equations are integro-differential equations with a large number of discretized degrees of freedom (in practice: the product of the number of chemical species taken into account by the number of size bins in a size-resolved approach). A key feature is related to the wide range of the characteristic timescales for condensation/evaporation. This induces the well known *stiffness* of the evolution system, which may be characterized by fast transient phases (the quick growth of small particles) and the need for appropriate numerical tools for time integration (implicit methods rather than explicit ones).

The numerical counterpart is a drastic increase of CPU time, even with the best available (implicit) solvers. An alternative approach is based on assumptions related to the equilibrium of condensation/evaporation. Many techniques have already been proposed. For a long time, condensation/evaporation has not been dynamically solved and a bulk equilibrium was supposed (Kim, Saxena, & Seinfeld, 1993; Nenes, Pandis, & Pilinis, 1998; Basset & Seinfeld, 1983; Saxena, Hudischewskyj, Seigneur, & Seinfeld, 1986). Size-resolved equilibrium (Pilinis & Seinfeld, 1987; Moya, Pandis, & Jacobson, 2002) or bulk equilibrium with size-resolved redistribution (Pandis, Wexler, & Seinfeld, 1993) have also been proposed. One very promising method is the so-called hybrid approach (Capaldo, Pilinis, & Pandis, 2000; Koo & Pandis, 2003) with a partition of the distribution into small particles (supposed to be at equilibrium) and large particles (given by condensation/evaporation dynamics).

These works have been mainly conducted in the framework of 3D modelling and, up to our knowledge, theoretical investigation has not been conducted before. The objective of this paper is to apply an appropriate theoretical framework (the theory of reduction for slow/fast systems) and to derive the appropriate reduced models. This article is therefore a follow-up of previous works devoted to the reduction of atmospheric chemistry: gas-phase chemistry (Sportisse & Djouad, 2000) and aqueous-phase chemistry (Sportisse & Djouad, 2003; Djouad, Sportisse, & Audiffren, 2003) have already been investigated. In the case of aerosol modelling, this is strongly related to the hybrid methods (Capaldo et al., 2000; Koo & Pandis, 2003).

In the first step, the objective of this article is not to propose an alternative to the currently used methods for 3D modelling: there are many reasons for uncertainty (lack of emission data, lack of size-resolved data, modelling of secondary organic aerosols) and, at this stage, minimizing the error related to equilibrium assumptions is probably not a crucial point. However, we think that this is relevant to give a common basis to these approaches and to use some tools that have already been used for similar problems. The focus of this article is then rather the methodology and the assessment of the validity of reduced models.

This article is organized as follows.

In the first section, we recall the underlying equations with a special attention paid to the lagrangian formulation of the condensation/evaporation process. The magnitude of timescales is also estimated. In the second section, we give the main features of slow/fast systems and we present the reducing methods and the application to aerosols. Some numerical tests are presented in the third section with a system of inorganic atmospheric aerosols based on the thermodynamic model Isorropia (Nenes et al., 1998). We also propose some appropriate methods for solving the reduced models, which appears to be particularly difficult to be integrated.

1. Condensation/evaporation for multicomponent aerosols

1.1. Notations and units

The aerosol model used for this work is the Size Resolved Aerosol Model (SIREAM). We refer to Debry (2004).

The physical processes that govern the aerosol dynamics are coagulation, condensation/evaporation (c/e in the following), nucleation and internal chemical reactions. The evolution of aerosols is then described by the general dynamic equation for aerosols (GDE), which couples all these processes.

We will focus on c/e. The internal chemical reactions are indeed usually omitted. Moreover, coagulation is also often neglected in urban simulations (Wexler, Lurmann, & Seinfeld, 1994). Another reason is that the numerical simulation of the GDE is often done by splitting the processes. In such a numerical framework we then focus on the condensation/evaporation step.

The aerosol populations are described by size distributions: a distribution for number concentration (n; in $\mathrm{m}^{-3}\,\mu\mathrm{g}^{-1}$) and a set of distributions for the n_s chemical species inside the aerosols (q_i for species X_i, i ranging from 1 to n_s; in $\mu\mathrm{g}\,\mathrm{m}^{-3}\,\mu\mathrm{g}^{-1}$).

Under the assumption of internal mixing (the distributions only depend on the aerosol size, not on the chemical composition), n and q_i may, for instance, be given as a function of aerosol mass m (in μg): $n(m,t)\,\mathrm{d}m$ represents the number concentration of aerosols whose mass ranges between m and $m+\mathrm{d}m$, at time t. The density distribution q_i for species X_i is such that $q_i = n \times m_i$ with m_i the mass of X_i in aerosols of mass m ($\sum_{i=1}^{i=n_s} m_i = m$).

The c/e equations for the aerosols are then given by

$$\frac{\partial n}{\partial t} = -\frac{\partial (I_0 n)}{\partial m}, \quad \frac{\partial q_i}{\partial t} = -\frac{\partial (I_0 q_i)}{\partial m} + I_i n, \tag{1}$$

where $I_i(m,t)$ (in $\mu\mathrm{g}\,\mathrm{s}^{-1}$) is the c/e rate of semi-volatile species X_i to aerosols of mass m. The total rate for one aerosol, usually referred as the growth rate I_0, is defined by $I_0(m,t) = \sum_{i=1}^{n_s} I_i(m,t)$.

These equations are written for $m \geqslant m_0$, with m_0 the smallest aerosol mass below which an aerosol is no longer stable. This mass is determined by the nucleation process.

The corresponding equations for gas-phase concentrations are given by the conservation of total mass during the c/e process. If c_i^{g} (in $\mu\mathrm{g}\,\mathrm{m}^{-3}$) is the gas-phase concentration of semi-volatile species X_i, the mass conservation equation can be written as $c_i^{\mathrm{g}} + \int_{m_0}^{\infty} q_i(m,t)\,\mathrm{d}m = K_i$ with K_i the total available mass for species X_i. In a similar way

$$\frac{\mathrm{d}c_i^{\mathrm{g}}}{\mathrm{d}t} = -\int_{m_0}^{\infty} I_i(m,t) n(m,t)\,\mathrm{d}m. \tag{2}$$

These equations are usually written in a logarithmic scale because the sizes lie on several orders of magnitude. For $x = \ln(m)$ we define the densities $n(x,t)$ and $q_i(x,t)$. As $n(x,t)\,\mathrm{d}x = n(m,t)\,\mathrm{d}m$ and $q_i(x,t)\,\mathrm{d}x = q_i(m,t)\,\mathrm{d}m$, we easily obtain $n(x,t) = mn(m,t)$ and $q_i(x,t) = mq_i(m,t)$. It is straightforward to obtain for these new densities

$$\frac{\partial n}{\partial t}(x,t) + \frac{\partial (H_0 n)}{\partial x} = 0, \quad \frac{\partial q_i}{\partial t}(x,t) + \frac{\partial (H_0 q_i)}{\partial x} = I_i n \tag{3}$$

with $H_0 = I_0/m$. For the gas-phase concentrations (with $x_0 = \ln m_0$),

$$c_i^{\mathrm{g}}(t) + \int_{x_0}^{\infty} q_i(x,t)\,\mathrm{d}x = K_i \quad \text{or} \quad \frac{\mathrm{d}c_i^{\mathrm{g}}}{\mathrm{d}t} = -\int_{x_0}^{\infty} I_i(\mathrm{e}^x, t) n(x,t)\,\mathrm{d}x. \tag{4}$$

In order to avoid too heavy notations, we have systematically used dry aerosol quantities. We refer to Debry (2004) for more details.

1.2. Sectional discretization and lagrangian formulation

The numerical discretization of the above equations is based on a lagrangian approach. This formulation is particularly appropriate in order to study the dynamical behaviour of aerosols (Jacobson & Turco, 1995; Kim & Seinfeld, 1990; Gaydos, Koo, Pandis, & Chock, 2003). Notice that the eulerian logarithmic formulations also leads to numerical diffusion (Sandu & Borden, 2003).

The aerosol distribution is discretized in n_b lagrangian bins $[\bar{x}^j, \bar{x}^{j+1}]$ indexed by j. The bounds $\bar{x}^j$ are defined by the so-called c/e characteristic curves:

$$\frac{\mathrm{d}\bar{x}^j}{\mathrm{d}t} = H_0(\bar{x}^j, t), \quad \bar{x}^j(0) = \bar{x}_0^j \tag{5}$$

with $\bar{x}_0^j$ the initial position at time $t=0$. *Provided that the* n_b+1 *curves cannot cross*, we can define integrated quantities over each bin:

$$N^j(t) = \int_{\bar{x}^j(t)}^{\bar{x}^{j+1}(t)} n(x,t)\,\mathrm{d}x, \quad Q_i^j(t) = \int_{\bar{x}^j(t)}^{\bar{x}^{j+1}(t)} q_i(x,t)\,\mathrm{d}x. \tag{6}$$

If we integrate (3) over each bin $j = 1, \ldots, n_b$:

$$\frac{dN^j}{dt} = \frac{d\bar{x}^{j+1}}{dt} n(\bar{x}^{j+1}, t) - \frac{d\bar{x}^j}{dt} n(\bar{x}^j, t) + \int_{\bar{x}^j}^{\bar{x}^{j+1}} \frac{\partial n}{\partial t}(x, t)\, dx$$
$$= (H_0 n)(\bar{x}^{j+1}, t) - (H_0 n)(\bar{x}^j, t) - \int_{\bar{x}^j}^{\bar{x}^{j+1}} \frac{\partial (H_0 n)}{\partial x}(x, t)\, dx = 0 \tag{7}$$

and we check that N^j remains constant under c/e. In the same way, the evolution of the integrated quantities Q_i^j are given by

$$\frac{dQ_i^j}{dt} = \int_{\bar{x}^j}^{\bar{x}^{j+1}} I_i(e^x, t) n(x, t)\, dx. \tag{8}$$

Note at this stage that Eq. (8) is still exact. The crucial point is that it does not provide a way for computing Q_i^j because a numerical quadrature has to be proposed for the integral: the number distribution $x \mapsto n(x, t)$ is not known inside each bin and the term $I_i(e^x, t)$ has to be approximated.

The simplest closure scheme for $n(x, t)$ is to use a constant function:

$$\text{for } x \in [\bar{x}^j, \bar{x}^{j+1}[, \quad n(x, t) \simeq \frac{N^j(t)}{\bar{x}^{j+1}(t) - \bar{x}^j(t)}. \tag{9}$$

The c/e growth $I_i(e^x, t)$ can also be approximated by a constant term, computed at the average mass of the aerosol bin defined as $\tilde{m}^j = \sum_{i=1}^{n_s} \tilde{m}_i^j$ with $\tilde{m}_i^j = Q_i^j / N^j$:

$$\text{for } x \in [\bar{x}^j, \bar{x}^{j+1}[, \quad I_i(e^x, t) \simeq I_i^j (= I_i(\tilde{m}^j, t)). \tag{10}$$

Eq. (8) is finally approximated by

$$\frac{dQ_i^j}{dt}(t) = N^j I_i^j. \tag{11}$$

For the gas phase, we easily obtain

$$c_i^g(t) + \sum_{j=1}^{n_b} Q_i^j(t) = K_i \quad \text{or} \quad \frac{dc_i^g}{dt} = -\sum_{j=1}^{n_b} I_i^j N^j. \tag{12}$$

At this stage, the integration of (11)–(12) may be performed in order to solve the c/e process. If a projection to a fixed size grid has to be done (this is for instance the case if the c/e step has been integrated in the framework of a splitting method applied to the GDE) the bounds in Eq. (5) still need to be solved. An alternative is to propose a closure scheme, which is usually done in practice. A classical closure scheme in the literature is $\bar{x}^j = (\tilde{x}^{j-1} + \tilde{x}^j)/2$, which is related to the geometric average of masses for adjacent bins ($\tilde{x}^j = \ln(\tilde{m}^j)$).

The aerosol model SIREAM uses the following closure scheme: we assume that the interpolation is not modified from time t to time $t + \Delta t$. If $\Delta\tilde{x}^j$ is defined as $\tilde{x}^j(t + \Delta t) - \tilde{x}^j(t)$, we compute for the internal bounds of bins ($j = 2, \ldots, n_b$):

$$\bar{x}^j(t + \Delta t) - \bar{x}^j(t) = (1 - \gamma)\Delta\tilde{x}^{j-1} + \gamma\, \Delta\tilde{x}^j, \quad \gamma = \frac{\bar{x}^j(t) - \tilde{x}^{j-1}(t)}{\tilde{x}^j(t) - \tilde{x}^{j-1}(t)}, \tag{13}$$

where $\tilde{x}^j(t)$, $\tilde{x}^{j-1}(t)$ and $\bar{x}^j(t)$ are known quantities. The bounds $\bar{x}^1$ and $\bar{x}^{n_b+1}$ can be extrapolated from the internal bounds (we omit the technical details for the sake of clarity).

1.3. Mass transfer

In order to close the above equations one has to define the c/e mass flux for species X_i in bin j:

$$I_i^j = \underbrace{2\pi D_i^g d_p^j f_c(K_{n_i}^j, \alpha_i)}_{a_i^j}(c_i^g - \eta_i^j(d_p^j)c_i^{eq}(\tilde{m}_1^j, \ldots, \tilde{m}_{n_s}^j)). \tag{14}$$

D_i^g is the air-diffusion coefficient of volatile species X_i. d_p^j is the aerosol wet diameter for bin j. $f_c(K_{n_i}^j, \alpha_i)$ is the correction function (Dahneke, 1983) due to noncontinuous effects, depending on Knudsen number $K_{n_i}^j$ and accomodation coefficient α_i. c_i^{eq} is the concentration near the aerosol surface, supposed to be at equilibrium with the aerosol mixture. η_i^j is the Kelvin effect correction.

The surface concentration can be obtained from thermodynamic equilibrium models, such as Isorropia (Pilinis, Capaldo, Nenes, & Pandis, 2000) for inorganics. A simplified model is used for organics (Bowman, Odum, Seinfeld, & Pandis, 1997). Furthermore, as equilibrium laws only depend on mass fraction, multiplying $\tilde{m}_i^j$ by any positive number β does not change the equilibrium concentrations: $c_i^{eq}(\beta\tilde{m}_1^j, \ldots, \beta\tilde{m}_{n_s}^j) = c_i^{eq}(\tilde{m}_1^j, \ldots, \tilde{m}_{n_s}^j)$, so that

$$c_i^{eq}(\tilde{m}_1^j, \ldots, \tilde{m}_{n_s}^j) = c_i^{eq}(Q_1^j, \ldots, Q_{n_s}^j). \tag{15}$$

By replacing the bulk and surface gas concentrations with their expression in Eqs. (12) and (15), Eq. (11) are modified as

$$\frac{dQ_i^j}{dt} = N^j a_i^j(t)\left(K_i - \sum_{j'=1}^{n_b} Q_i^{j'} - \eta_i^j c_i^{eq}(Q_1^j, \ldots, Q_{n_s}^j)\right). \tag{16}$$

This is the evolution system we study in the following. Nevertheless, this system is not yet completely closed as the transfer rate depends on aerosol diameter, to be computed according to integrated quantities Q_i^j. We also apply a mass flux limitation as in Pilinis et al. (2000). We refer to Debry (2004) for more details.

1.4. Timescales

Such models are characterized by a widespread of timescales and we now derive a rough estimation of these timescales.

As $dQ_i^j/dt = N^j I_i^j = I_i^j/\tilde{m}_i^j Q_i^j$, a first approximation of the timescale τ_i^j for the species X_i in aerosol bin j is

$$\tau_i^j = \frac{\tilde{m}_i^j}{|I_i^j|}. \tag{17}$$

These timescales strongly depend on the aerosol size. On the one hand $\tilde{m}_i^j$ is proportional to the aerosol volume $\tilde{m}_i^j \sim (d_p^j)^3$ by assuming a constant aerosol density. On the other hand, the c/e transfer rate I_i^j is proportional to the aerosol diameter in the continuous regime (for $K_{n_i} \ll 1$, $I_i^j \sim d_p^j$) and to its square in the free molecular regime (for $K_{n_i} \gg 1$, $I_i^j \sim (d_p^j)^2$), where K_n is the Knudsen number. Finally, we get for the timescales

$$K_{n_i} \gg 1 \Rightarrow \tau_i^j \sim d_p^j, \quad K_{n_i} \ll 1 \Rightarrow \tau_i^j \sim (d_p^j)^2. \tag{18}$$

This indicates that the aerosol timescales may range over many orders of magnitude (as the aerosol diameters do). This behaviour is illustrated in Fig. 1 through the evolution of τ_i^j with respect to diameter. The initial conditions are those defined in Section 3.1. In order to compute an accurate solution we have used $n_b = 50$ bins.

We now investigate the reduction of such systems in the next section.

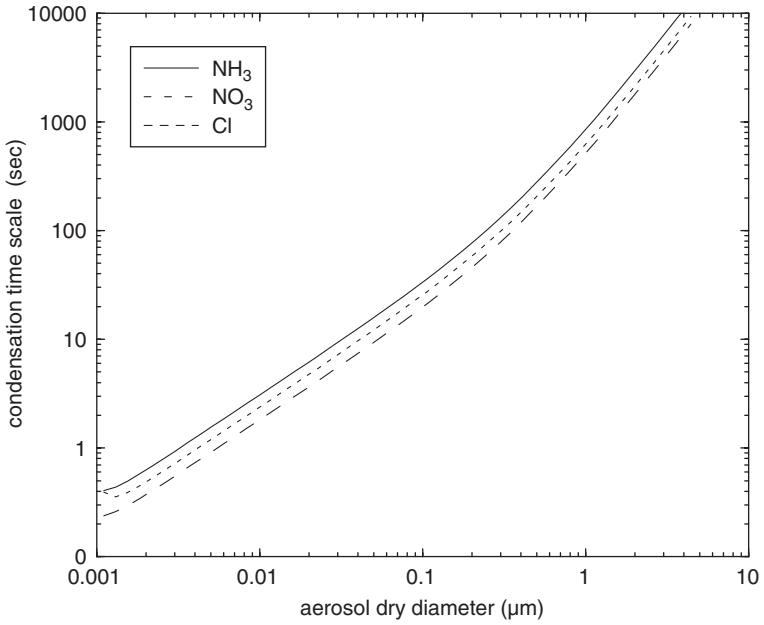

Fig. 1. Evolution of the aerosol timescales with respect to aerosol diameter.

2. Reduction of the c/e equation

2.1. Reduction methods

2.1.1. Slow/fast systems

Slow/fast systems are characterized by the *possible partitioning* of the degrees of freedom into a set of *slow components* and a set of *fast components*, z_s and z_f, respectively. The evolution model is therefore under the form

$$\frac{dz_s}{dt} = f(z_s, z_f), \quad \varepsilon\frac{dz_f}{dt} = g(z_s, z_f), \quad z_s(0) = (z_s)_0, \quad z_f(0) = (z_f)_0, \tag{19}$$

where ε is a small positive parameter which describes the ratio of fast timescales to slow timescales. ε is of course not given in practice (unless an appropriate scaling of the initial model is performed) but the key assumption is that *we should be able* to write the model under this form (appropriate for understanding what happens). f and g describe the dynamics for z_s and z_f, respectively.

The key result is that the initial model given by Eq. (19) may be approximated up to first order in ε by a so-called *reduced model*, after a fast transient phase whose length is of magnitude ε:

$$\frac{dz_s}{dt} = f(z_s, z_f), \quad g(z_s, z_f) = 0, \quad z_s(0) = (z_s)_0. \tag{20}$$

The evolution of the fast variables is then given by an equilibrium with the slow variables: this is of course an extension of the so-called quasi-steady state assumption of chemical kinetics. The key point is that this does not depend on the initial conditions.

The equilibrium is supposed to give a solution $z_f = h(z_s)$, which gives some constraints for the initial partitioning into slow and fast components. The reduced model (20) is not stiff and can be easily integrated with explicit methods under the condition that the constraint $g(z_s, z_f) = 0$ may be solved.

2.1.2. Some numerical criteria for partitioning

In practice, the models are not under the nice form (19). As said before, scaling the initial variables is supposed to lead to such a form. This is of course not usable as such and some numerical criteria can be used in order to perform

the partitioning of the initial variables. We now assume that the model is under the general form:

$$\frac{\mathrm{d}z}{\mathrm{d}t} = F(z), \quad z(0) = z_0, \quad z \in \mathbf{R}^{n_z} \tag{21}$$

and we want to generate the associated model (19) by partitioning z.

(1) A first method is based on the study of the eigenvalues of the Jacobian matrix $J = \partial F/\partial z$. The stiffness of the model (the slow/fast behaviour) is deeply associated with the wide range of magnitudes covered by the eigenvalues: the characteristic timescales are indeed defined as the inverse of the absolute values of the eigenvalues.
Let $\lambda_{n_z} \leqslant \lambda_{n_z-1}, \ldots, \lambda_1 \leqslant 0$ be the negative eigenvalues of the model. We assume that there is a gap such that $\lambda_{n_z-p+1} \ll \lambda_{n_z-p}$, which defines $n_z - p$ slow modes and p fast modes. Let $\vec{u}_k$ be the orthonormal eigenvector associated with λ_k. We define the subspace of fast variables (resp. slow variables) V_f (resp. V_s) through

$$V_\mathrm{f} = \mathrm{span}(\vec{u}_{n_z-p+1}, \ldots, \vec{u}_{n_z}), \quad V_\mathrm{s} = \mathrm{span}(\vec{u_1}, \ldots, \vec{u}_{n_z-p}). \tag{22}$$

A good criterion for assessing whether a component z_l is a slow or a fast degree of freedom is therefore to compute its projection onto V_f and V_s. We define the norms of its fast (resp. slow) projection p_f (resp. $p_\mathrm{s} = 1 - p_\mathrm{f}$) through

$$(p_\mathrm{f})_l = \sum_{k=n_z-p+1}^{k=n_z} ((\vec{u}_k)_l)^2, \quad (p_\mathrm{s})_l = \sum_{k=1}^{k=n_z-p} ((\vec{u}_k)_l)^2 \tag{23}$$

with $(\vec{u})_l$ the lth component of $\vec{u}$. If $(p_\mathrm{f})_l \gg (p_\mathrm{s})_l$, then the component z_l may be considered as a fast component.
The advantage of this method is its generality and the complete description of the dynamical behaviour of the model through the eigenvalues and the eigenvectors of the linearized model. The drawback is the CPU time needed for computing the eigenvalues.

(2) A second method is based on the so-called QSSA ratio associated to z_l. We assume that the time evolution of z_l may be written under the so-called loss/production form $\mathrm{d}z_l/\mathrm{d}t = P_l - C_l$, with $P_l \geqslant 0$ and $C_l \geqslant 0$ the production and loss terms, respectively. The QSSA ratio is then defined by

$$(I_\mathrm{QSSA})_l = \frac{|P_l - C_l|}{P_l + C_l}. \tag{24}$$

If $(I_\mathrm{QSSA})_l \leqslant \varepsilon_c$, with ε_c a small value provided by the model user, z_l is supposed to be a fast component. Notice that this criterion is very easy to implement. In practice, ε_c is set to values ranging from 1% to 10%. This criterion is a way for scaling the system and checking the validity of the algebraic constraint of the reduced model $g(z_\mathrm{s}, z_\mathrm{f}) = 0$.

2.2. Application to the c/e equations

We define the vector z of length $n_z = n_\mathrm{s} \times n_\mathrm{b}$ in the following way: for $1 \leqslant j \leqslant n_\mathrm{b}$ and $1 \leqslant i \leqslant n_\mathrm{s}$, we compute $l = (i-1)n_\mathrm{b} + j$ and we define $z_l = Q_i^j$. In the following, a general index l will be systematically associated to a bin index j and a species index i such that $l = (i-1)n_\mathrm{b} + j$.

The evolution of z is then given by $\mathrm{d}z/\mathrm{d}t = F(z)$ with

$$F_l = N^j \underbrace{a_i^j(t) \left(\overbrace{K_i - \sum_{j'=1}^{n_\mathrm{b}} Q_i^{j'}(t)}^{c_i^\mathrm{g}} - \eta_i^j c_i^\mathrm{eq}(Q_1^j, \ldots, Q_{n_\mathrm{s}}^j) \right)}_{I_i^j}. \tag{25}$$

The partitioning criteria have to be adapted:

(1) The first method requires the Jacobian matrix J of the system (25), which is defined for $(l_1, l_2) \in \{1, \dots, n_z\}^2$ as $J_{l_1 l_2} = \partial F_{l_1}/\partial z_{l_2}$. For $l_1 = (i_1 - 1)n_b + j_1$ and $l_2 = (i_2 - 1)n_b + j_2$, we have $J_{l_1 l_2} = N^{j_1}(\partial I_{i_1}^{j_1}/\partial Q_{i_2}^{j_2})$. After some tedious manipulations, we obtain

$$\begin{aligned} J_{l_1 l_2} &= N^{j_1}\left[\frac{\partial a_{i_1}^{j_1}}{\partial Q_{i_2}^{j_2}}(c_{i_1}^{g} - \eta_{i_1}^{j_1}(c_{i_1}^{eq})^{j_1}) + a_{i_1}^{j_1}\left(\frac{\partial c_{i_1}^{g}}{\partial Q_{i_2}^{j_2}} - \frac{\partial(\eta_{i_1}^{j_1}(c_{i_1}^{eq})^{j_1})}{\partial Q_{i_2}^{j_2}}\right)\right] \\ &= \underbrace{N^{j_1} a_{i_1}^{j_1}\frac{\partial c_{i_1}^{g}}{\partial Q_{i_2}^{j_2}}}_{\text{linear}} + \underbrace{N^{j_1}\left(\frac{\partial I_{i_1}^{j_1}}{\partial Q_{i_2}^{j_2}}\right)_{c_{i_1}^{g}=\text{cste}}}_{\text{nonlinear}}, \end{aligned} \tag{26}$$

where the bulk gas-phase concentration $c_{i_1}^{g}$ is kept constant along the derivation in the nonlinear part. The mass conservation equation (12) provides an easy derivation of the linear part:

$$\frac{\partial c_{i_1}^{g}}{\partial Q_{i_2}^{j_2}} = \begin{cases} 0 & i_1 \neq i_2, \\ -1 & i_1 = i_2. \end{cases} \tag{27}$$

The nonlinear part needs to differentiate the thermodynamic equilibrium, which is difficult due to thresholds and discontinuities of thermodynamics. In practice, we approximate this (highly) nonlinear part by finite differences:

$$\frac{\partial I_{i_1}^{j_1}}{\partial Q_{i_2}^{j_2}} \simeq \frac{I_{i_1}^{j_1}(\dots, Q_{i_2}^{j_2}(1 + \varepsilon_{jac}), \dots) - I_{i_1}^{j_1}(\dots, Q_{i_2}^{j_2}, \dots)}{Q_{i_2}^{j_2}\varepsilon_{jac}}, \tag{28}$$

where ε_{jac} is a small constant (of magnitude 10^{-8} in our tests).
We can then compute the eigenvalues of J and the corresponding projections to the slow and fast subspaces, once a cutting value λ_c is defined among the eigenvalues.

(2) According to the expression of I_i^j in Eq. (25) the QSSA ratio for each component z_l is

$$(I_{QSSA})_l = \frac{|c_i^{g} - \eta_i^j (c_i^{eq})^j|}{c_i^{g} + \eta_i^j (c_i^{eq})^j}. \tag{29}$$

Once the partitioning has been made, the reduced system is under the form (20). In the general case, one given species in one given bin may be at equilibrium, independent of the other species in the same bin. In practice, we want to use equilibrium models bin per bin. We will then aggregate the previous criteria (for instance I_{QSSA}) by summing over the species in one given bin. The fast components z_f will then be solved by an equilibrium model $g(z_s, z_f) = 0$, which corresponds in practice to the so-called "forward mode" of thermodynamic models such as Isorropia (Nenes et al., 1998, see below).

2.3. Some numerical methods

On the basis of the previous criteria, we now assume that there exists a cut-off diameter below which all bins are at equilibrium. We label this bin by j_c. The equilibrium model g is then defined for bins $1 \leqslant j \leqslant j_c$ by

$$1 \leqslant i \leqslant n_s, \quad K_i - \sum_{j'=1}^{n_b} Q_i^{j'} - \eta_i^j c_i^{eq}(Q_1^j, \dots, Q_{n_s}^j) = 0. \tag{30}$$

This defines for each bin j at equilibrium an algebraic system of n_s unknown variables $(Q_1^j, \dots, Q_{n_s}^j)$.

The thermodynamic models take into account only one aerosol bin. Some appropriate numerical methods have therefore to be developed for solving the reduced model over many bins. We now present the so-called bulk approach

(Pandis et al., 1993) in which all bins are merged and redistributed after equilibrium, and the general size-resolved approaches (Jacobson, Tabazadeh, & Turco, 1996, with a specific iterative algorithm).

2.3.1. Bulk equilibrium

The bulk equilibrium approach developed by Pandis et al. (1993) is based on the merging of all the bins supposed to be at equilibrium. Let $B_i = \sum_{j=1}^{j_c} Q_i^j$ be the mass of species X_i in bins at equilibrium and $\tilde{K}_i = K_i - \sum_{j=j_c+1}^{n_b} Q_i^j$ the available mass for gas-phase and bins at equilibrium.

We can then write the system (30) for $1 \leqslant j \leqslant j_c$ as

$$1 \leqslant i \leqslant n_s, \quad \tilde{K}_i = B_i + \eta_i^j c_i^{eq}(Q_1^j, \ldots, Q_{n_s}^j). \tag{31}$$

The bulk equilibrium approach consists in merging all the bins at equilibrium into a single bulk bin at equilibrium, supposed to meet

$$1 \leqslant i \leqslant n_s, \quad \tilde{K}_i = B_i + c_i^{eq}(B_1, \ldots, B_{n_s}) \tag{32}$$

Eq. (32) can be directly solved by a thermodynamic model. This is for instance the case with the *forward mode* of Isorropia (the input is $\tilde{K}_i$, the outputs are B_i^{eq} and c_i^{eq} that meet Eq. (32)). The bulk values B_i^{eq} are usually distributed over the bins at equilibrium ($1 \leqslant j \leqslant j_c$) through the following algorithm:

$$1 \leqslant i \leqslant n_s, \quad (Q_i^j)^{eq} = Q_i^j + f_i^j (B_i^{eq} - B_i), \quad f_i^j = \frac{a_i^j N^j}{\sum_{j'=1}^{j_c} a_i^{j'} N^{j'}}, \tag{33}$$

where B_i and Q_i^j are the values defined at the beginning of the current timestep. Let us briefly investigate the required assumptions:

- (A1) The Kelvin effect can be neglected.
- (A2) The mass fractions are uniform over the fast bins $1 \leqslant j \leqslant j_c$: for $1 \leqslant i \leqslant n_s$, $Q_i^j / \sum_{i'=1}^{n_s} Q_{i'}^j$ does not depend on j. This implies the same result for B_i.

  The equilibrium value may then be computed independently of the bins. For any $1 \leqslant j \leqslant j_c$:

$$1 \leqslant i \leqslant n_s, \quad c_i^{eq}(Q_1^j, \ldots, Q_{n_s}^j) = c_i^{eq}(B_1, \ldots, B_{n_s}). \tag{34}$$

- (A3) The variation within one time step $[0, \Delta t]$ for the c/e coefficients $a_i^j(t)$ can be neglected.

According to assumptions (A1) and (A2), Eqs. (31) and (32) are equivalent. In order to justify the redistribution algorithm (33), we derive from Eq. (16):

$$1 \leqslant i \leqslant n_s, \quad 1 \leqslant j \leqslant j_c, \quad \frac{dQ_i^j}{dt} = N^j a_i^j(t)(c_i^g - c_i^{eq}) \tag{35}$$

which gives the following evolution for B_i:

$$1 \leqslant i \leqslant n_s, \quad \frac{dB_i}{dt} = \left(\sum_{j=1}^{j_c} N^j a_i^j(t) \right) (c_i^g - c_i^{eq}). \tag{36}$$

The integration of (35)–(36) over $[0, \Delta t]$ gives under (A3):

$$1 \leqslant j \leqslant j_c: \quad (Q_i^j)^{eq} - Q_i^j = a_i^j N^j \Delta c_i, \quad (B_i)^{eq} - B_i = \left(\sum_{j=1}^{j_c} a_i^j N^j \right) \Delta c_i \tag{37}$$

with $\Delta c_i = \int_0^{\Delta t} (c_i^g(t') - c_i^{eq}(B_1(t'), \ldots, B_{n_s}(t'))) \, dt'$. This is exactly the redistribution algorithm.

2.3.2. Size-resolved equilibrium

We give in this section two classical methods:

(1) A first approach is related to a fixed point algorithm.
The basic idea is to apply a thermodynamic model sequentially for each bin (Jacobson et al., 1996). The loop over all bins has to be performed until the concentrations reach a stable value.
Let us describe one iteration. The equilibrium is solved from bin j_c to bin 1, i.e., from the slowest bin to the fastest bin (which is logical because the fast components have to be computed after the slow ones):

$$1 \leqslant i \leqslant n_s, \quad K_i^{j_c} = Q_i^{j_c} + c_i^g, \tag{38}$$

where we have defined $K_i^j = K_i - \sum_{j'=1, j' \neq j}^{j_c} Q_i^{j'}$. We then get the equilibrium concentrations $(Q_i^{j_c})^{eq}$ and $(c_i^{eq})^{j_c}$ by using the forward mode of the equilibrium model. The gas-phase concentrations are then used for the next equilibrium calculation for bin $j_c - 1$:

$$1 \leqslant i \leqslant n_s, \quad K_i^{j_c-1} = Q_i^{j_c-1} + (c_i^{eq})^{j_c}, \tag{39}$$

where $K_i^{j_c-1}$ is computed by taking into account $(Q_i^{j_c})^{eq}$. This provides the aerosol equilibrium concentrations $(Q_i^{j_c-1})^{eq}$ and the new gas-phase equilibrium concentrations $(c_i^{eq})^{j_c}$. This iterative algorithm may be used until $j = 1$, which ends a first iteration.
This iterative process ensures mass conservation.

(2) A drawback of the former method is that a fixed point algorithm is known to fail for stiff algebraic systems, for the same reason that implicit methods are advocated rather than explicit methods for time integration.
Another way to perform size-resolved equilibrium (30) is then to apply well-known numerical techniques for nonlinear systems (Press, Vetterling, Teukolsky, & Flannery, 2001), such as Newton–Raphson methods. We use in practice a quasi-Newton method, the so-called BFGS minimization algorithm (Byrd, Lu, Nocedal, & Zhu, 1995).

3. Numerical tests

We have applied the former algorithms to a box model simulation. We have chosen to focus on one typical situation. The results are similar for other cases and we have chosen not to report them because it does not add any new informations. However, we are aware that 3D simulations will encounter many other situations but the focus is not on this point.

3.1. Numerical setup

The number distribution is a log-normal distribution with two modes:

$$n(\ln(d_p)) = \frac{1}{\sqrt{2\pi}} \sum_{k=1}^{2} \frac{N_t^k}{\ln(\sigma_g^k)} \exp\left[-\frac{1}{2} \left(\frac{\ln(d_p) - \ln(d_g^k)}{\ln(\sigma_g^k)} \right)^2 \right], \tag{40}$$

where N_t^k, σ_g^k and d_g^k are, respectively, the aerosol number concentration, the standard deviation and the mean aerosol diameter for each mode k: $N_t^1 = 38\,000\,\mathrm{cm}^{-3}$, $N_t^2 = 5400\,\mathrm{cm}^{-3}$, $\sigma_g^1 = 1.6$, $\sigma_g^2 = 1.8$, $d_g^1 = 0.013\,\mu\mathrm{m}$ and $d_g^2 = 0.069\,\mu\mathrm{m}$.

The aerosol diameters range from $d_{\min} = 0.001\,\mu\mathrm{m}$ to $d_{\max} = 5.0\,\mu\mathrm{m}$. We use $n_b = 15$ bins.

We start from a uniform aerosol composition over bins with only inorganic species (SOA are not taken into account). The mass percentages for all bins are 30% for Na and NH_3, 20% for Cl and NO_3 and 0% for sulfate.

The initial gas-phase concentrations are $c_{SO_4} = c_{NH_3} = c_{NO_3} = c_{Cl} = 2.0\,\mu\mathrm{g\,m}^{-3}$.

The accomodation coefficient α is set to 0.1 for all species (as a standard value for modelling atmospheric aerosols).

The simulation time is set to $\Delta t = 1000\,\mathrm{s}$, which is a typical splitting timestep in 3D Chemistry-Transport Models.

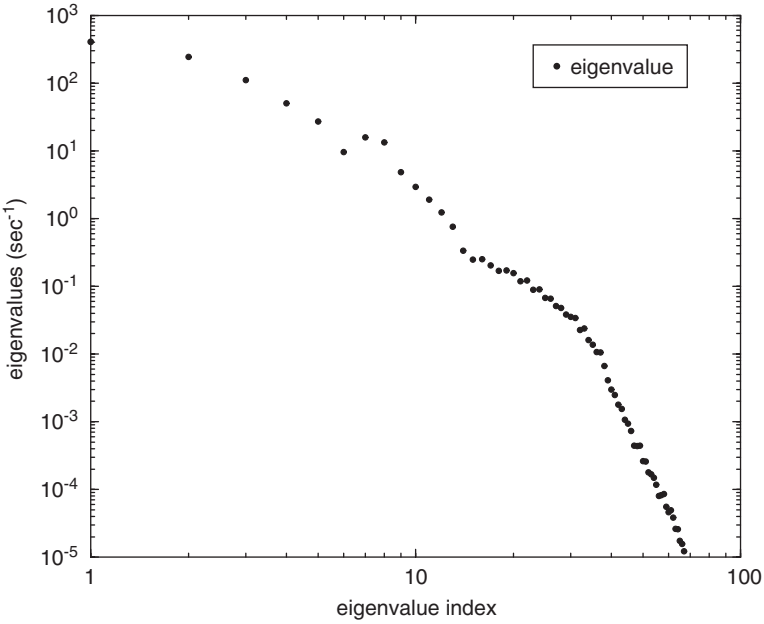

Fig. 2. Distribution of eigenvalues at $t = 0.5$ s.

A reference solution is computed on the basis of the exact model (without reduction) with the explicit solver ETR (an explicit trapezoidal rule). Subcycling is used for time integration: the timestep is computed on the basis of an adaptive strategy with ETR by comparing the first-order and the second-order estimations of the solution (we omit the technical details for the sake of clarity). We use a strong constraint in order to have an accurate reference solution.

For the reduced models, the slow components are solved with ETR while the fast components are solved with the numerical methods given above. In order to compare the solutions the same adaptive strategy is used in all simulations.

3.2. Results and discussion

We first illustrate the dynamical behaviour of the aerosol distribution and we compare the reducing methods in a second part.

3.2.1. Dynamical behaviour of the reference solution

The eigenvalues at time $t = 0.5$ s are plotted in Fig. 2. They range over many orders of magnitude, which illustrates the stiffness.

Figs. 3 and 4 show which species and bins are concerned with stiff eigenvalues. We have plotted the ratio p_f/p_s for a cut-off eigenvalue $\lambda_c = 1$ and 0.1, respectively. This is a way for determining the cut-off diameter (d_c), below which all aerosol bins are set at equilibrium. When λ_c is decreased the number of bins at equilibrium is larger.

The QSSA ratio is plotted in Fig. 5 at the same time $t = 0.5$ s. It gives the same behaviour as obtained through the study of eigenvalues.

As aerosol dynamics is a relaxation process towards equilibrium between aerosols and gas, the cut-off diameter d_c should increase with time. The time evolution of the cut-off diameter is given in Fig. 6 for various values of ε_c values (as defined in Section 2.1.2). The jumps are related to the time integration (with subcycling timesteps).

3.2.2. Benchmark of reducing methods

The objective of this section is to benchmark the reducing methods in order to evaluate the sensitivity with respect to the reduction assumptions and to the numerical algorithms.

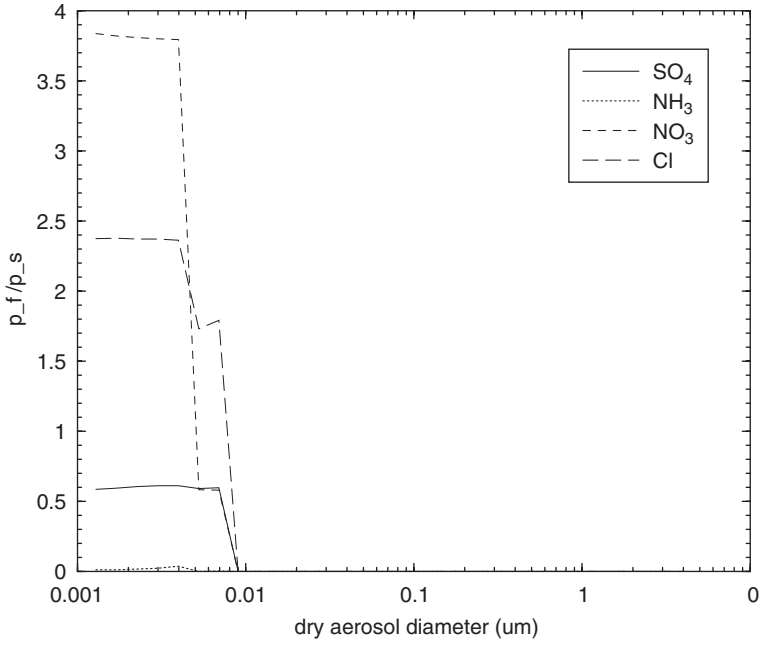

Fig. 3. Distribution of slow/fast components at $t = 0.5$ s with $\lambda_c = 1$.

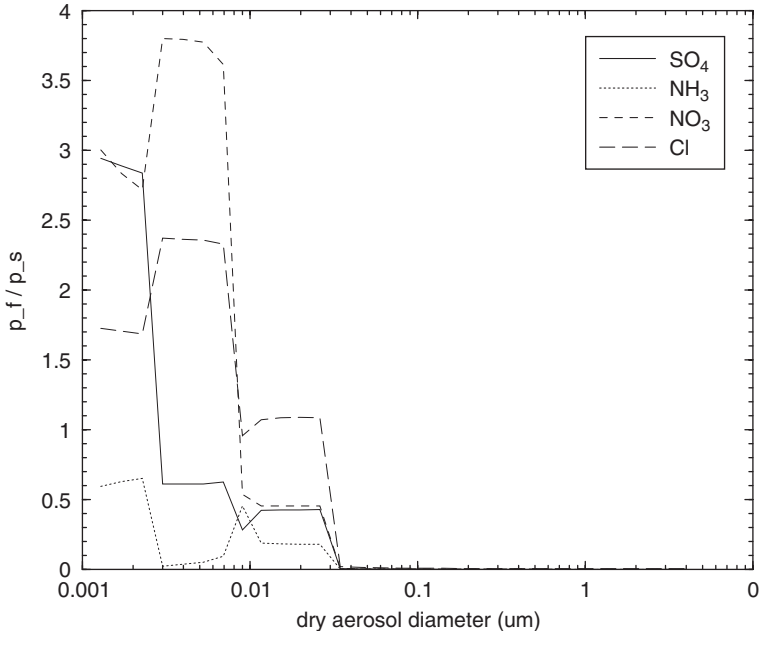

Fig. 4. Distribution of slow/fast components at $t = 0.5$ s with $\lambda_c = 0.1$.

The absolute and relative errors between the reference solution and the reduced solution, $\mathrm{err_a}$ and $\mathrm{err_r}$, respectively, are computed as follows:

$$\mathrm{err_a} = \sqrt{\sum_{i,j=1}^{n_s,n_b} ((q_i^j)^{\mathrm{ref}} - (q_i^j)^{\mathrm{red}})^2}, \quad \mathrm{err_r} = \sqrt{\sum_{i,j=1}^{n_s,n_b} \left(\frac{(q_i^j)^{\mathrm{ref}} - (q_i^j)^{\mathrm{red}}}{\max(q_{\mathrm{tol}}, (q_i^j)^{\mathrm{ref}}, (q_i^j)^{\mathrm{red}})} \right)^2} \tag{41}$$

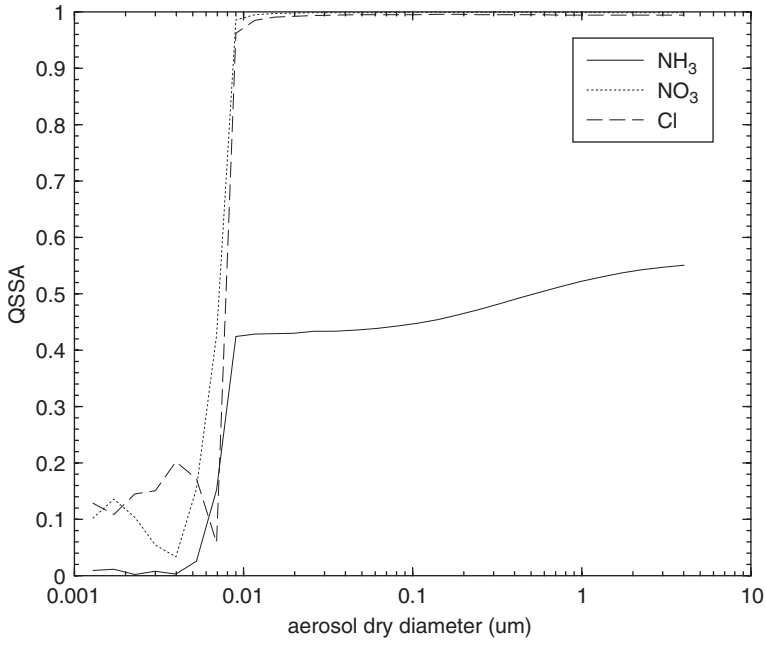

Fig. 5. QSSA ratio at $t = 0.5$ s.

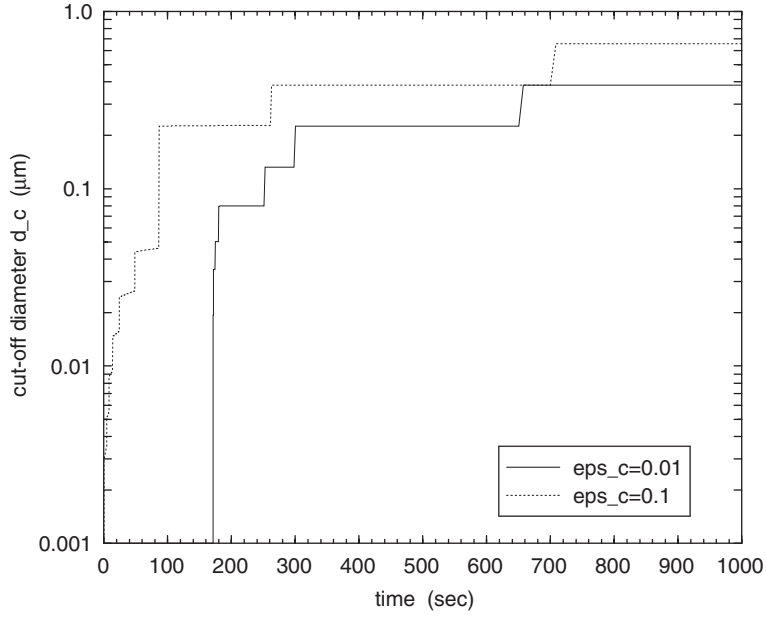

Fig. 6. Time evolution of the cut-off diameter d_c for different values of ε_c.

with the threshold $q_{\text{tol}} = 10^{-15}\ \mu\text{g m}^{-3}$. $(q_i^j)^{\text{ref}}$ and $(q_i^j)^{\text{red}}$ are the uniform distributions computed from the integrated quantities at the end of the computation as $q_i^j = Q_i^j/(\bar{x}^{j+1} - \bar{x}^j)$.

We have investigated the impact of the following choices:

- reducing method (bulk equilibrium versus size-resolved equilibrium);

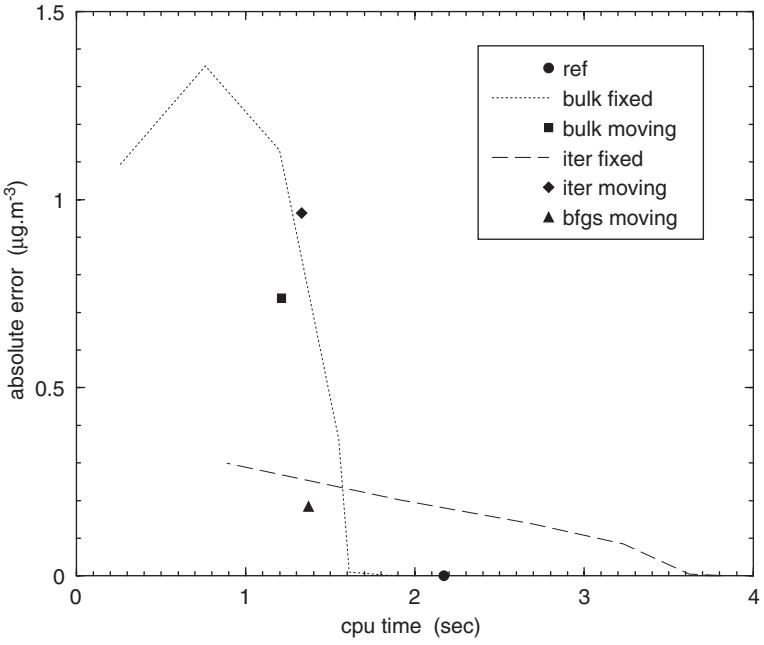

Fig. 7. Absolute error versus CPU time for different reduction strategies.

- partitioning criterion (fixed cut-off diameter versus moving cut-off diameter);
- numerical solver used for solving the size-resolved equilibrium (fixed point algorithm versus BFGS).

Notice that the errors associated to reduced models may come from the reducing method itself (a modelling error) or from the equilibrium solver itself (a numerical error).

Figs. 7 and 8 show the dependence of the absolute error and of the relative error, respectively, with respect to CPU time for the following reducing methods and strategies:

- *ref*: reference solution;
- *bulk fixed*: bulk equilibrium method for various fixed d_c;
- *bulk moving*: bulk equilibrium method with moving d_c;
- *iterative fixed*: iterative method for various fixed d_c;
- *iterative moving*: iterative method with moving d_c;
- *bfgs moving*: BFGS method with moving d_c.

For the "fixed" methods we have chosen a fixed value for the cut-off bin j_c at the beginning of the simulation: bins below j_c (including j_c itself) are considered as bins at equilibrium during the simulation. Each bin (among the n_b bins) has been used as the cut-off bin, which generates a curve of n_b points in the figures.

For the "moving" methods the cut-off diameter is set to 0.001 µm at the beginning of the simulation and evolves according to the QSSA ratio. The parameter ε_c is set to 0.01. This only defines one run (that is to say one point in the figures).

The *bulk fixed* curve shows that the bulk equilibrium method is less and less efficient as the fixed cut-off diameter is increased, which is logical (the reduced model is less and less accurate).

As the "moving cut-off diameter" strategy defines the most accurate reduced model, the errors should be mainly due to the equilibrium solver itself. Therefore, the *bulk moving* method improves the efficiency of the bulk equilibrium solver: the point related to *bulk moving* is on the left part of the line related to the *bulk fixed* method (this means that for a given CPU time, it is more accurate; or that for a given accuracy, it is less CPU expensive).

On the contrary to the *bulk fixed* curve, the *iterative fixed* curve smoothly increases as the fixed cut-off diameter increases (the slope is much lower). This is logical because it is supposed to be a more accurate method. This illustrates the strong sensitivity of the accuracy for the *bulk fixed* method with respect to the cut-off diameter.

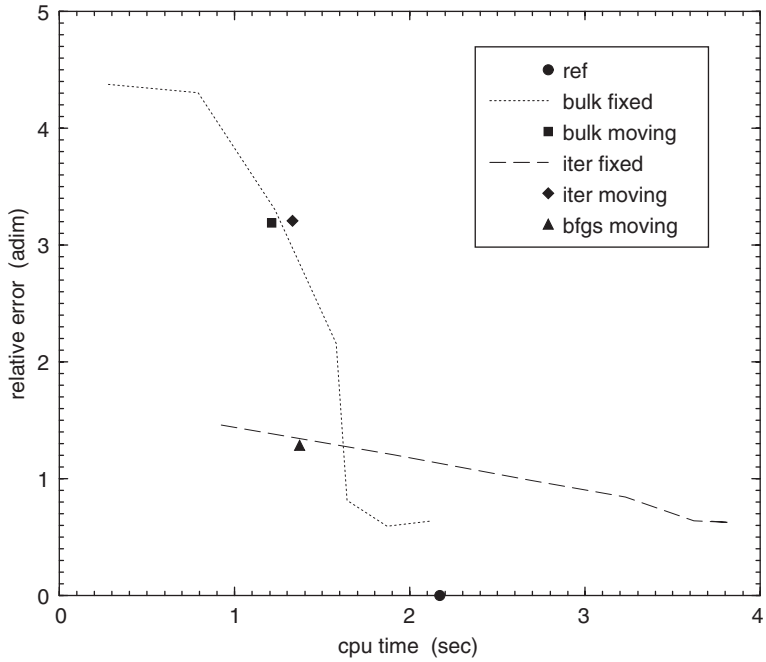

Fig. 8. Relative error versus CPU time for different reduction strategies.

The use of the "moving cut-off diameter" strategy with the size-resolved equilibrium solved with the fixed point algorithm does not improve the results as for the bulk equilibrium method. The comparison between the *iterative fixed* curve and the *iterative moving* point (the point is on the right part of the curve) indicates that the numerical solver used (the fixed point algorithm) probably generates significant errors and instabilities, which anneals the gain in accuracy due to the moving strategy.

The comparison of *bfgs moving* to *bulk moving* and *iterative moving* indicates that BFGS is the most efficient solver for moving strategies (it is on the left part of both curves). This was expected as this method is supposed to minimize the modelling error and the numerical error. Nevertheless this method has appeared to be highly sensitive to the values of ε_c (tests not reported here). It fails to solve the equilibrium when this parameter is increased or when the cut-off diameter is fixed (that is why we have not reported a curve in this case): in both cases, the reduced system is wrong and this may illustrate the difficulty to solve a reduced model that is not physically justified. In this respect this method appears to be less robust.

4. Conclusion

We have investigated in this article the theoretical basis for reducing condensation/evaporation models for aerosols. We have tested the sensitivity of the results with respect to the reduction hypothesis and to the numerical approaches used for solving the reduced models. The results (obtained in a box model simulation for inorganic species) have illustrated a large sensitivity to the reducing strategy.

As pointed out in Capaldo et al. (2000) the stiffness of the aerosol models lies in smallest bins. The hybrid methods in which the smallest bins are solved by a gas/aerosol equilibrium model are then the most efficient method. In this framework, we have also proposed a criterion for adapting the cut-off diameter, which seems to be more efficient than using an arbitrarily fixed cut-off diameter.

The conclusions of these tests are those expected: we recover the most accurate solutions among the reduced models and the most accurate numerical solvers. This also illustrates the difficulty of getting a robust solution. Our tests indicate the lack of robustness of many reduced models. The compromise between a small error due to reduction and

the numerical stability of the associated model is hard to achieve. In this context, moving strategies appear to be more appropriate for bulk approaches.

Future works will be devoted to the extension to 3D cases with a Chemistry-Transport Model.

Acknowledgements

We thank Professor Spyros Pandis, from Carneggie-Mellon-University, for his help and for the access to his models (especially Isorropia).

This work has been partially supported by the French Research Program Primequal-Predit, in the framework of the PAM project (Multiphase Air Pollution).

References

Basset, M., & Seinfeld, J. (1983). Atmospheric equilibrium model of sulfate and nitrate aerosol. *Atmospheric Environment*, *17*, 2237–2252.

Bowman, F., Odum, J., Seinfeld, J., & Pandis, S. (1997). Mathematical model for gas-particle partitioning of secondary organic aerosols. *Atmospheric Environment*, *31*(23), 3921–3931.

Byrd, H., Lu, P., Nocedal, J., & Zhu, C. (1995). A limited memory algorithm for bound constrained optimization. *SIAM Journal of Scientific Computing*, *16*(5), 1190–1208.

Capaldo, K., Pilinis, C., & Pandis, S. (2000). A computationally efficient hybrid approach for dynamic gas/aerosol transfer in air quality models. *Atmospheric Environment*, *34*, 3617–3627.

Dahneke, B. (1983). *Theory of dispersed multiphase flow*. New York: Academic Press.

Debry, E. (2004). *Numerical simulation of the general dynamic equation.* Ph.D. thesis, Ecole Nationale des Ponts et Chaussées.

Djouad, R., Sportisse, B., & Audiffren, N. (2003). Reduction of multiphase atmospheric chemistry. *Journal of Atmospheric Chemistry*, *46*, 131–157.

Gaydos, T., Koo, B., Pandis, S., & Chock, D. (2003). Development and application of an efficient moving sectional approach for the solution of the atmospheric aerosol condensation/evaporation equations. *Atmospheric Environment*, *37*(23), 3303–3316.

Jacobson, M., Tabazadeh, A., & Turco, R. (1996). Simulating equilibrium within aerosols and nonequilibrium between gases and aerosols. *Journal of Geophysical Research*, *101*(D4), 9079–9091 American Geophysical Union.

Jacobson, M., & Turco, R. (1996). Simulating condensational growth evaporation and coagulation of aerosols using a combined moving and stationary size grid. *Aerosol Science and Technology*, *22*, 73–92.

Kim, Y., Saxena, P., & Seinfeld, J. (1993). Atmospheric gas-aerosol equilibrium i. thermodynamic model. *Aerosol Science and Technology*, *19*, 157–181.

Kim, Y., & Seinfeld, J. (1990). Simulation of multicomponent aerosol condensation by the moving sectional method. *Journal of Colloid and Interface Science*, *135*(1), 185–199.

Koo, B., & Pandis, S. (2003). Evaluation of the equilibrium, dynamic, and hybrid aerosol modelling approaches. *Aerosol Science and Technology*, *37*, 53–64.

Moya, M., Pandis, S., & Jacobson, M. (2002). Is the size distribution of urban aerosols determined by thermodynamic equilibrium? An application to southern California. *Atmospheric Environment*, *36*(14), 2349–2365.

Nenes, A., Pandis, S., & Pilinis, C. (1998). Isorropia: A new thermodynamic equilibrium model for multicomponent inorganic aerosols. *Aquatic Geochemistry*, *4*, 123–152.

Pandis, S., Wexler, A., & Seinfeld, J. (1993). Secondary organic aerosol formation and transport—ii. predicting the ambient secondary organic aerosol size distribution. *Atmospheric Environment*, *27A*(15), 2403–2416.

Pilinis, C., Capaldo, K., Nenes, A., & Pandis, S. (2000). Madm—a new multi-component aerosol dynamic model. *Aerosol Science and Technology*, *32*, 482–502.

Pilinis, C., & Seinfeld, J. (1987). Continued development of a general equilibrium model for inorganic multicomponent atmospheric aerosols. *Atmospheric Environment*, *21*(11), 2453–2466.

Press, W., Vetterling, W., Teukolsky, S., & Flannery, B., 2001. *Numerical recipes in fortran 77*, (2nd ed.) Vol. 1. Cambridge: Cambridge University Press.

Sandu, A., & Borden, C. (2003). A framework for the numerical treatment of aerosol dynamics. *Applied Numerical Mathematics*, *45*, 475–497.

Saxena, P., Hudischewskyj, A., Seigneur, C., & Seinfeld, J. (1986). A comparative study of equilibrium approaches to the chemical characterization of secondary aerosols. *Atmospheric Environment*, *20*, 1471–1483.

Seinfeld, J., & Pandis, S. (1998). *Atmospheric chemistry and physics*. New York: Wiley-Interscience.

Sportisse, B., & Djouad, R. (2000). Reduction of chemical kinetics in air pollution modelling. *Journal of Computational Physics*, *164*, 354–376.

Sportisse, B., & Djouad, R. (2003). Mathematical investigation of mass transfer for atmospheric pollutants into a fixed droplet with aqueous chemistry. *Journal of Geophysical Research Atmospheres*, *108*(D2), 4073.

Wexler, A., Lurmann, W., & Seinfeld, J. (1994). Modelling urban and regional aerosols—i. model development. *Atmospheric Environment*, *28*, 531–546.